ISSN 0020-1685, Inorganic Materials, 2015, Vol. 51, No. 1, pp. 1–4. © Pleiades Publishing, Ltd., 2015.
Original Russian Text © Sh.A. Mirsagatov, I.B. Sapaev, Zh.T. Nazarov, 2015, published in Neorganicheskie Materialy, 2015, Vol. 51, No. 1, pp. 3–6.

Ultrasonic Annealing of Surface States in the Heterojunction of a *p*-Si/*n*-CdS/n^+-CdS Injection Photodiode

Sh. A. Mirsagatov[a], I. B. Sapaev[a], and Zh. T. Nazarov[b]

[a] *Fizika–Solntse Research and Production Association, Physicotechnical Institute, Academy of Sciences of Uzbekistan, ul. Bodomzor-iuli 2b, Tashkent, 100084 Uzbekistan*

[b] *Navoi State Mining Institute, Yuzhnaya ul. 27a, Navoi, 210100 Uzbekistan*

e-mail: mohim@inbox.ru

Received January 26, 2014

Abstract—We have studied the effect of ultrasonic processing on the electrical and photoelectric properties of a *p*-Si/*n*-CdS/n^+-CdS injection photodiode. The results demonstrate that ultrasonic processing of such photodiodes reduces the density of surface states at the interface of their heterojunction as a result of defect annealing. This increases the spectral and integrated sensitivities of the photodiodes.

DOI: 10.1134/S0020168515010148

There is now conclusive evidence that ultrasonic processing (USP) influences the defect structure and electrical properties of semiconductors [1–6]. USP has the following advantages over thermal annealing and irradiation:

1. Ultrasonic waves are absorbed in solids predominantly in regions where the periodicity of their crystal lattice is distorted, so ultrasonication has a more local effect.

2. The use of ultrasonic waves of various polarizations and types allows one to improve the selectivity of USP.

3. Varying the ultrasound frequency, one can induce resonance transformations in the defect system.

The purpose of this work was to investigate the effect of USP on the electrical and photoelectric properties of a *p*-Si/*n*-CdS/n^+-CdS injection photodiode. Such photodetectors were produced and studied previously [7, 8]. The structure is taken to be under forward or reverse bias when the *p*-Si contact is positively or negatively biased, respectively. Analysis of current–voltage (I–V) data demonstrates that the structure exhibits rectifying behavior, with a rectification ratio (defined as the ratio of the forward current to the reverse current at a constant bias voltage $V_b = 20$ V) $K \simeq 10^5$. Figure 1 shows I–V curves of the *p*-Si/*n*-CdS/n^+-CdS structure in the dark and under illumination before and after USP at a power density of 1 W/cm^2 and a frequency $f = 2.5$ MHz for 15 min. According to our results, USP has no effect on the relationship between the forward and reverse currents in the structure in the dark and under illumination and only increases the current at a given bias voltage (Fig. 1).

The structures were illuminated by the output of an LG-75 laser at a wavelength of 0.625 μm and incident power densities from 10 μW/cm^2 to 0.75 mW/cm^2 or by an incandescent lamp which was essentially identical in parameters to a standard lamp with 1 lm corresponding to 9.1×10^{-3} W of power of electromagnetic radiation in the visible range [9]. Both in the dark and under illumination, the forward current increases by ≃20% and the reverse current increases about twofold.

Tables 1 and 2 list the spectral (S_λ) and integrated (S_{int}) sensitivities at various white light and laser output ($\lambda = 0.625$ μm) intensities, incident power densities, and bias voltages under forward and reverse bias before and after USP. As seen from Table 1, USP increases S_{int} and S_λ under forward bias by about 20%, independent of the white light intensity, inci-

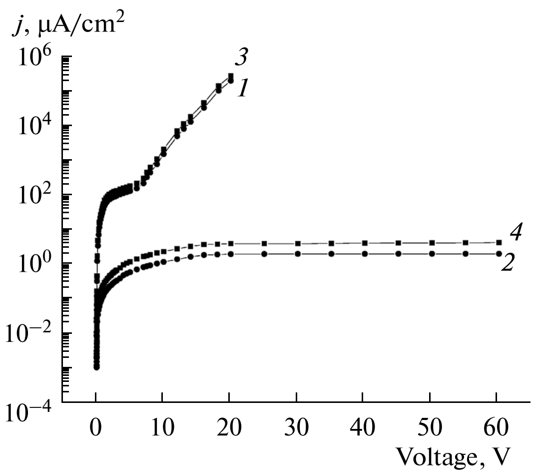

Fig. 1. Semilog plot of dark I–V data for the *p*-Si/*n*-CdS/n^+-CdS structure: (*1*) forward I–V curve before USP, (*2*) reverse I–V curve before USP, (*3*) forward I–V curve after USP, (*4*) reverse I–V curve after USP.

Table 1. Influence of illuminance (E), laser power density (P), forward bias voltage (V), and USP on the integrated sensitivity (S_{int}) and spectral sensitivity (S_λ)

E, lx	V, V	S_{int}, A/W		P, μW/cm^2	S_λ, A/W	
		before USP	after USP		before USP	after USP
white light				laser output		
0.05	5	0.2×10^4	0.316×10^4	0.7	36	42.85
	10	4.2×10^4	5×10^4		550	660
	15	3.21×10^5	3.85×10^5		3057	3669
	20	4.47×10^6	9.76×10^6		50358	60428
0.1	5	0.2×10^4	0.195×10^4	10	13.3	16
	10	2.6×10^4	3.1×10^4		200	240
	15	1.87×10^5	2.24×10^5		1120	1344
	20	3×10^6	3.62×10^6		23356	28027.2
1	5	0.2×10^3	0.23×10^3	50	7.4	8.86
	10	3.32×10^3	3.98×10^3		121.5	145.8
	15	1.98×10^4	2.37×10^4		778.7	934.5
	20	3.4×10^5	4.1×10^5		8326	9992
10	5	0.2×10^2	0.24×10^2		4.56	5.47
	10	4×10^2	4.75×10^2	100	75.24	90.29
	15	2.31×10^3	2.77×10^3		440.25	528.3
	20	4.5×10^4	5.4×10^4		4483.2	5379.84

dent laser power density, and bias voltage. Under reverse bias, USP increases the spectral and integrated sensitivities of the photodetector by more than a factor of 2 (Table 2). Moreover, the absolute values of S_{int} and S_λ under reverse bias are about four orders of magnitude lower than those under forward bias. At the same time, the spectral sensitivity considerably exceeds the S_λ of an ideal photodetector. For example, $S_\lambda = 0.5$ A/W [10] at $\lambda = 0.625$ μm for an ideal photodetector, whereas the spectral sensitivity of the structure under investigation is 1.31 A/W at this wavelength, $P = 10$ μW/cm^2, and $V = 5$ V. At higher bias voltages, S_λ is even higher. The relatively low values of S_{int} and S_λ under reverse bias can be understood in

Table 2. Influence of illuminance (E), laser power density (P), reverse bias voltage (V), and USP on the integrated sensitivity (S_{int}) and spectral sensitivity (S_λ)

E, lx	V, V	S_{int}, A/W		P, μW/cm^2	S_λ, A/W	
		before USP	after USP		before USP	after USP
white light				laser output		
0.1	5	40.1	80.2	10	1.31	2.62
	10	47.36	94.72		1.883	3.766
	60	76	152		7	13.8

terms of the physical processes in the base of the structure and the formation of a sublinear portion in its I–V characteristic. Adirovich et al. [11] and Karageorgii-Alkalaev and Leiderman [12] analyzed in detail the formation of a sublinear portion in I–V characteristics, which is due to opposite drift and diffusion flows in the high-resistance base of the structure. The presence of an extended sublinear portion in the reverse I–V characteristic of the p-Si/n-CdS/n^+-CdS structure indicates electron injection from the p-Si/n-CdS heterojunction to the high-resistance base (n-CdS) and suggests that n-CdS/n^+-CdS is an ideal homojunction whose energy barrier height increases with increasing applied reverse bias voltage (with the n^+-CdS layer positively biased) [9], which leads to the accumulation of nonequilibrium minority carriers (holes) near the n-CdS/n^+-CdS homojunction and produces diffusion flows opposite to the drift and diffusion flows from the p-Si/n-CdS heterojunction. As first shown by Adirovich et al. [11] and Karageorgii-Alkalaev and Leiderman [12], opposite diffusion and drift flows lead to "injection depletion" of the base region and their mutual compensation occurs. The sublinear current–voltage behavior in a wide range of bias voltages ($V \simeq$ 10–60 V) indicates that the region of mutual compensation of the drift and diffusion flows of nonequilibrium carriers becomes broader and that the resistance of the base and the electric field strength in the base increase, thereby increasing the ambipolar drift velocity. The above experimental data can be accounted for by the fact that the forward current in the structure under investigation is limited primarily by recombination processes, which are due to the surface states in the lower half of the band gap, and that the reverse current is determined by the surface states in the upper half of the band gap of silicon at the interface of the p-Si/n-CdS heterojunction. If the density of surface states (N_{ss}) in the upper half of the band gap far exceeds that in the lower half, USP is more effective in eliminating the surface states. To validate this statement, we investigated the capacitance–voltage (C–V) characteristic of the structure under consideration.

AC capacitance–voltage characteristics allow one to gain information about interfaces. The present C–V data indicated the formation of a metal–insulator–semiconductor (MIS) structure in our samples. The density of surface states in the MIS structure was evaluated by a standard procedure from the shift of the measured C–V characteristic relative to a calculated characteristic [13]. Figure 2 shows the measured (curve *1*) and calculated (*2*) capacitance–voltage curves of a typical injection photodetector based on the p-Si/n-CdS/n^+-CdS structure. The measured capacitance–voltage curve was obtained at a frequency $f = 10$ kHz and room temperature. The surface potential (ψ_s) at a given bias voltage was determined as described previously [14]. Figure 3 shows N_{ss} as a function of ψ_s. The $N_{ss}(\psi_s)$ curve has a higher density of surface states at a positive surface potential. At $\psi_s = -0.24$ eV, the density of surface states is $\simeq 6 \times 10^{11}$ cm^{-2}, in agreement with data reported by Tregulov [15], who indicated only the integrated density of surface states. The N_{ss} in the lower half of the band gap is far lower than that in the upper half: $N_{ss} \simeq 9.5 \times 10^9$ cm^{-2} at $\psi_s = 0.08$ eV and $N_{ss} \simeq 1.9 \times 10^{10}$ cm^{-2} at $\psi_s = 0.48$ eV.

Therefore, the effective density of surface states in the lower half of the band gap is low and varies little over an energy separation of $\simeq 0.48$ eV from midgap. The present experimental data confirm that there is a p-Si/n-CdS heterojunction with low N_{ss} even though cadmium sulfide and silicon differ in lattice parameter by more than 7% [16]. The reason for this is that the heterojunction has an intermediate layer which smooths the difference in lattice parameter between cadmium sulfide and silicon. The intermediate layer may consist of a solid solution between the semiconductors or of SiO_x, CdO_x, and SO_x, which form during the fabrication of the n-CdS/p-CdS heterojunction [8].

Capacitance measurements before and after USP confirm that the mechanism of electrical transport in the structure is interrelated with the surface states of the p-Si/n-CdS heterojunction.

Since USP reduces the density of surface states in the lower half of the band gap (Fig. 3, curve *2*) by 18–20%, the forward current decreases by roughly the same amount both in the dark and under illumination. The result is that, after USP, $N_{ss}(\psi_s)$ in the upper half of the band gap varies in a complex way. The variation of N_{ss} with ψ_s after USP indicates (Fig. 3, curve *2*) that the density of midgap surface states decreases by about a factor of 2, whereas the density of surface states far away from midgap (more precisely, at $\psi_s = -0.24$ eV) decreases by just 17%. Therefore, defects that act as recombination centers are eliminated more rapidly, so the reverse current increases by about a factor of 2 both in the dark and under illumination. Thus, USP increases S_{int} and S_λ under forward bias by about 20%, independent of the white light intensity, incident laser power density, and bias voltage (Table 1). Under reverse bias, USP increases the spectral and integrated sensitivities of the photodetector by about a factor of 2 (Table 2).

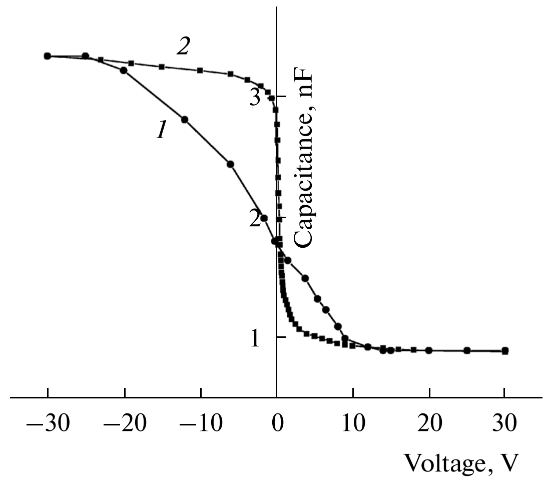

Fig. 2. (*1*) Measured and (*2*) calculated C–V curves of the p-Si/n-CdS/n^+-CdS structure at $f = 10$ kHz and $T = 300$ K.

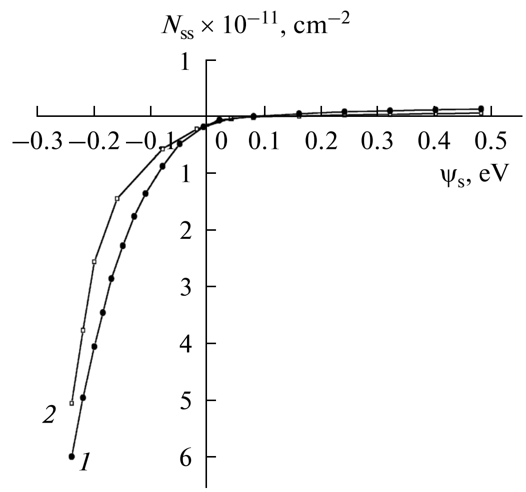

Fig. 3. Effective density of surface states as a function of surface potential (*1*) before and (*2*) after USP.

In conclusion, it is worth noting that the density of surface states in the p-Si/n-CdS heterojunction plays a key role in determining the spectral and integrated sensitivities of the injection photodetector based on the p-Si/n-CdS/n^+-CdS structure.

USP reduces the density of surface states on the interface of the p-Si/n-CdS heterojunction and increases the spectral and integrated sensitivities of injection photodetectors based on the p-Si/n-CdS/n^+-CdS structure under both forward and reverse bias. As a result, S_{int} and S_λ increase by about a factor of 2 under reverse bias and by ≃20% under forward bias.

REFERENCES

1. Baranskii, P.I., Belyaev, A.E., Koshirenko, S.M., et al., A mechanism behind the effect of ultrasonic processing on carrier mobility in semiconductor solid solutions, *Fiz. Tverd. Tela* (Leningrad), 1990, vol. 32, no. 7, pp. 2159–2161.
2. Ostrovskii, I.V., Steblenko, L.P., and Nadtochii, A.B., Ultrasound-induced surface hardening of dislocation-free silicon, *Semiconductors*, 2000, vol. 34, no. 3, pp. 251–254.
3. Zaveryukhina, E.B., Zaveryukhina, N.N., Lezilova, L.N., Zaveryukhin, B.N., et al., Acoustostimulated expansion of the short-wavelength sensitivity range of AlGaAs/GaAs solar cells, *Tekh. Phys. Lett.*, 2005, vol. 31, no. 1, pp. 27–32.
4. Olikh, O.Ya., Features of dynamic acoustically induced modification of photovoltaic parameters of silicon solar cells, *Semiconductors*, 2011, vol. 45, no. 6, pp. 798–804.
5. Davletova, A. and Karazhanov, S.Zh., Open-circuit voltage decay transient in dislocation-engineered, *J. Phys. D: Appl. Phys.*, 2008, vol. 41, no. 165, pp. 107–110.
6. Pashaev, I.G., Effect of various treatments on Schottky diode properties, *Semiconductors*, 2012, vol 46, no. 8, pp. 1085–1087.
7. Sapaev, I.B., Electrical and photoelectric properties of Au–pSi–nCdS–n^+CdS heterostructures, *Dokl. Akad. Nauk Uzb.*, 2013, no. 2, pp. 27–29.
8. Mirsagatov, Sh.A. and Sapaev, I.B., Injection photodiode based on a photosensitive polycrystalline CdS film, *IV Mezhdunarodnaya konferentsiya po aktual'nym problemam molekulyarnoi spektroskopii kondensirovannykh sred* (IV Int. Conf. on Critical Issues in Molecular Spectroscopy of Condensed Media), Samarkand, 2013, pp. 157–158.
9. Frish, E., *Opticheskie metody izmerenii* (Optical Measurement Techniques), Leningrad: Leningrad. Gos. Univ., 1976, part 1, p. 126.
10. Ambrozyak, A., *Konstruktsiya i tekhnologiya poluprovodnikovykh fotoelektricheskikh priborov* (Design and Technology of Photoelectric Semiconductor Devices), Moscow: Sovetskoe Radio, 1970, p. 392.
11. Adirovich, E.I., Karageorgii-Alkalaev, P.M., and Leiderman, A.Yu., *Toki dvoinoi inzhektsii v poluprovodnikakh* (Double Injection Currents in Semiconductors), Moscow: Sovetskoe Radio, 1978, p. 126.
12. Karageorgii-Alkalaev, P.M. and Leiderman, A.Yu., *Fotochuvstvitel'nost' poluprovodnikovykh struktur s glubokimi primesyami* (Photosensitivity of Semiconductor Structures Containing Deep Impurities), Tashkent: FAN, 1981, p. 200.
13. Sze, S.M., *Physics of Semiconductor Devices*, New York: Wiley, 1981, vol. 1. Translated under the title *Fizika poluprovodnikovykh priborov*, Moscow: Mir, 1984, vol. 1, p. 386.
14. Mirsagatov, Sh.A. and Uteniyazov, A.K., Injection photodiode based on p-CdTe film, *Tech. Phys. Lett.*, 2012, vol. 38, no. 1, pp. 34–37.
15. Tregulov, V.V., Determination of the density of surface states of CdS/Si(p) from analysis of capacitance–voltage characteristics, *Izv. Vyssh. Uchebn. Zaved. Povolzhsk. Reg.*, 2012, vol. 23, no. 3, pp. 124–132.
16. Milnes, A.G. and Feucht, D.L., *Heterojunctions and Metal–Semiconductor Junctions*, New York: Academic, 1972. Translated under the title *Geteroperekhody i perekhody metall-poluprovodnik*, Moscow: Mir, 1975, p. 425.

Translated by O. Tsarev